Received: 26 July 2020 | Revised: 9 September 2020 | Accepted: 20 October 2020

DOI: 10.1111/joa.13353

ORIGINAL PAPER

ANATOMICAL SOCIETY Journal of Anatomy WILEY

Sound production, hearing sensitivity, and in-depth study of the sound-producing muscles in the cowfish (*Lactoria cornuta*)

Eric Parmentier[1] | **Erica Marucco Fuentes**[2] | **Morgane Millot**[1] | **Xavier Raick**[1] | **Marc Thiry**[2]

[1]Laboratory of Functional and Evolutionary Morphology, AFFISH-RC, FOCUS, University of Liège, Liège, Belgium

[2]Laboratory of Cellular and Tissular Biology, GIGA-Neurosciences, Cell Biology L3, University of Liège, Liège, Belgium

Correspondence
Eric Parmentier, AFFISH-RC, FOCUS, University of Liège, Institut de Chimie - B6C, Sart Tilman, Liège 4000, Belgium.
Email: E.Parmentier@uliege.be

Funding information
Fonds De La Recherche Scientifique - FNRS, Grant/Award Number: T.0192.20

Abstract

The ability to produce sounds has been reported in various Ostraciidae but not deeply studied. In some *Ostracion* species, two different sound-producing muscles allow these boxfishes to produce two different kinds of sounds in a sequence. This study investigates sound production in another Indo-Pacific species, the longhorn cowfish *Lactoria cornuta* that also possesses two pairs of sonic muscles associated with the swim bladder: extrinsic sonic muscles (ESMs) and intrinsic sonic muscles (ISMs). The cowfish produces two kinds of sounds called hums and clicks. Hums are made of trains of low amplitude pulses that last for long periods of time, suggesting that they are produced by fatigue-resistant muscles, whereas clicks correspond to shorter sounds with greater amplitude than the hums, suggesting that they result from more powerful contractions. Ultra-structural differences are found between extrinsic and intrinsic sonic muscles. According to features such as long sarcomeres, long I-bands, a high number of mitochondria, and a proliferation of sarcoplasmic reticulum (SR), ESMs would be able to produce fast, strong, and short contractions corresponding to clicks (the shortest sounds with the greatest amplitude). ISMs have the thinnest cells, the smallest number of myofilaments that have long I-bands, the highest volume of mitochondria, and well-developed SR supporting these muscles; these features should generate fast and prolonged contractions that could correspond to the hums that can be produced over long periods of time. A concluding figure shows clear comparisons of the different fibers that were studied in *L. cornuta*. This study also compared the call features of each sound with the cowfish's hearing ability and supports *L. cornuta* was more sensitive to frequencies ranging between at least 100 and 400 Hz with thresholds of 128–143 dB re 1 μPa over this range, meaning that they are sensitive to the frequencies produced by conspecifics.

KEYWORDS

acoustic, audition, communication, hearing, histology, Ostraciidae, sonic muscle, swim bladder

1 | INTRODUCTION

Sound production is a characteristic shared by many fishes and has been described in many different families (Fine & Parmentier, 2015). Sound-producing mechanisms have evolved independently in different distant taxa meaning that they show the widest range of sound production apparatuses among vertebrates (Ladich & Fine, 2006; Fine & Parmentier, 2015). Within all vocal teleosts, some

species are quite exceptional because they can use different kinds of mechanisms. The mochokid, pimelodid, and doradid catfish can use both their pectoral fins to produce stridulatory sounds (Heyd & Pfeiffer, 2000; Parmentier, Bouillac, et al., 2010; Parmentier, Fabri, et al., 2010; Tellechea et al., 2011) and swim bladder-associated muscle to produce drumming sounds (Boyle et al., 2014, 2015; Ladich, 1997). In Balistidae, sounds can be produced by alternate sweeping movements of the pectoral fins which push modified scales against the swim bladder wall (Parmentier et al., 2017; Raick et al., 2018) but also by the dorsal fin (Schneider, 1961). Some piranhas can produce brief sounds when they snap their jaws (Millot et al., 2011) and low-frequency harmonic sounds using high-speed muscles that ventrally surround the swim bladder (Ladich & Bass, 2005; Markl, 1971; Mélotte et al., 2016, 2019). However, both kinds of sounds are not produced simultaneously in these taxa and the mechanisms are clearly different. There are also taxa (Carapidae, Holocentridae, Pomacentridae, Zeidae, etc.) in which a single specimen is able to produce different kinds of sounds using the same mechanism. In this case, sound variations are mainly due to modifications at the level of the pulse period (Mann & Lobel, 1995; Onuki & Somiya, 2004; Parmentier, Bahri, et al., 2018; Parmentier et al., 2016; Parmentier, Fine, et al., 2018).

Ostraciidae are known as boxfishes because of their cubic or tetrahedral shaped body that is almost completely covered by a bony shell or carapace formed of thick hexagonal modified conjoined plates. Sound production in different species of Ostraciidae has been sporadically reported but their sounds were not physically described (Fish & Mowbray, 1970). The bluespotted boxfish *Ostracion immaculatus* can produce a grating sound by grinding its upper and lower teeth (Uchida, 1934), whereas vibrations were heard in *Lactophrys trigonus* (Bridge, 1904; Fish, 1948). In the thornback cowfish *Lactoria fornasini*, the sounds produced are high-pitched hums that are used to synchronize spawning (Moyer, 1979). In *Ostracion meleagris*, Lobel identified three different sounds that are produced during spawning, competition, and agonistic behavior (Lobel, 1996). More recently, sounds and, for the first time, the associated mechanisms have been described in the boxfishes *Ostracion cubicus* and *O. meleagris* (Parmentier et al., 2019). These species are able to produce two sounds in a sequence. Both species produce long weak hums that are sometimes interspersed with loud clicks. Interestingly, two distinct pairs of sonic muscles were described. Extrinsic vertical muscles originate on the vertebral column and attach to the swim bladder. Perpendicularly and below these muscles, longitudinal intrinsic muscles cover the swim bladder, allowing a distinct second sound-producing mechanism (Parmentier et al., 2019). The periodicity of the hums and clicks supports that they are the result of rhythmic muscle contractions. The action of sonic muscles induces the production of sounds with a fundamental frequency ranging from 100 to 200 Hz, placing them among the fastest muscles present in vertebrates (Fine et al., 2001; Loesser et al., 1997). Preliminary histological investigation of the sound production muscles has been performed in *O. cubicus* and *O. meleagris*. Sonic muscles of both species had characteristics of high speed muscles but not enough information was present to unambiguously associate a sonic muscle to a sound type (Parmentier et al., 2019). The loud clicks could even be the result of the simultaneous contraction of both kinds of muscles.

The longhorn cowfish *Lactoria cornuta* (Linnaeus, 1758) is found in shallow waters of the Ind-Pacific. It is usually solitary and territorial but is haremic during the reproduction period. Sounds in this species, closely related to *Ostracion* spp. (Santini et al., 2013), were never previously recorded and provide a nice opportunity to expand the study of the acoustic biology of Ostraciidae. We aimed to conduct a multidisciplinary approach to *L. cornuta* bioacoustics. First, we described their sounds and the corresponding sound-producing mechanism. Then, we conducted a deep investigation of their sound-producing muscles, that is, extrinsic and intrinsic sonic muscles, to reveal distinct features and assess their functions. Third, the cowfish's hearing ability was determined to make comparisons with call features.

2 | MATERIALS AND METHODS

2.1 | Fish specimens

All specimens (total length, TL: 60–170 mm) were purchased in an aquarium store, stocked separately in tanks (99 × 39 × 25 cm and 74 × 38 × 35 cm) at 26 ± 1°C and were maintained on a 12 h light/dark cycle. There is no sexual dimorphism and the sex was not determined. Within a tank, fish were separated by perforated barriers to avoid fighting between specimens. The tanks were equipped with external filters, internal heaters, and bubblers for the oxygenation of the water. Fish were fed with mussels three times a week.

2.2 | Sound collection and analysis

After an acclimatization period of 10 days, 15 specimens were recorded with a hydrophone (HTI Min-96, Long Beach, USA; sensitivity: −163.7 dB re. 1 V μPa^{-1}; flat frequency response range between 2 Hz and 30 kHz) connected to a recorder TASCAM DR-05 (TEAC, Wiesbaden, Germany). The hydrophone was positioned in the center of the tank. Each specimen was recorded by being gently held, by hand, at 3 ± 1 cm from the hydrophone. Specimens were recorded in different tanks (74 × 38 × 36 cm, 78 × 29 × 30 cm, 99 × 39 × 26 cm) with the water temperature maintained at 27 ± 1°C. The effects of reverberation and resonance can induce potential artifacts in the characteristics of sounds recorded in small glass tanks (Akamatsu et al., 2002). The computed resonant frequencies of the recording tanks varied from 3.05 to 3.75 kHz and were much higher than the dominant frequency. The sounds were digitized on a mono-channel at 44.1 kHz with a 16 bit-resolution and then they were sub-sampled at 3000 Hz. A high-pass filter at 50 Hz was then applied to remove frequencies smaller than 50 Hz, corresponding to the majority of the background noise. Only sounds with a good signal to noise

ratio (SNR), that is, with at least 10 dB of difference between the dominant amplitude of the sound and the amplitude corresponding to the same frequency in the background noise, were used. Sounds were analyzed using Avisoft SAS-Lab Pro 5.2 (Avisoft Bioacoustics, Germany). Temporal features were measured on oscillograms, and the frequency was obtained from power-spectra. The sound parameters measured were: (1) the dominant frequency (Hz), (2) the sound pressure level (in dB re 1 μPa @ 3 ± 1 cm), (3) the sound duration (ms), (4) the number of peaks in the sound, and (5) the period, that is, the duration between the onset of two successive repetitions (ms) of the same pattern. In sounds longer than one second, ten periods were randomly measured.

2.3 | Morphology and histology

Five *Lactoria cornuta* specimens were euthanized in a tricaine methanesulfonate solution (CAS: 886-86-2). Three specimens were fixed in 5% formalin for two days and transferred to 70% ethyl alcohol. These fish were dissected and examined using a Wild M10 binocular microscope (Leica Microsystems GmbH, Germany) equipped with a camera lucida. One specimen (TL: 115 mm) was immediately dissected to sample the two muscles attached to the swim bladder and two typical skeletal muscles that were used as a control. The first control muscle is a part of the epaxial muscle (EM), a long superficial muscle located just below the carapace, originating dorsally on the caudal part of the skull and inserting on the caudal peduncle. The second control muscle is the adductor mandibulae A_2 (AM) that joins the suspensorium to the mandible. The muscle samples were soaked in glutaraldehyde 2.5% (CAS: 111-30-8) and small sub-samples (1 cm × 1 cm) were extracted. These fragments were divided into smaller pieces (0.5 m × 1 cm) and fixed in 2.5% glutaraldehyde in Sorensen's buffer 0.1 M solution at 4°C for 24 h. After three washes in Sorensen's buffer, samples were post-fixed for 60 min in 2% osmium tetroxide (CAS: 20816-12-0) and dehydrated through graded ethanol–propylene oxide series then embedded in epoxy resin (SPI-PON 812, SPI-CHEM). The resin was then polymerized at 60°C for 48 hours. Semi-thin (1 μm) and ultra-thin sections (60–70 nm) were cut using a diamond knife (Diatome) mounted in an ultramicrotome (Ultracut S Leica). Semi-thin sections of each muscle were stained with a toluidine blue solution and observed under an Olympus Provis Light Microscope at 40× magnification to select the areas to be sampled for Transmission Electron Microscopy (TEM), and 20 longitudinal fields were randomly photographed for each muscle to analyze the width of the myocytes. Ultra-thin sections were contrasted in the dark for 15 min in uranyl acetate solution (CAS: 6159-44-0), and for 15 min in lead citrate solution (CAS: 14450-60-3). For ultrastructural analyses, random fields of these pieces were examined under a Jeol TEM JEM-1400 Transmission Electron Microscope at 80 kV, and random fields were photographed using an 11 megapixel camera system (Quemesa, Olympus). For each muscle, 21 fields were microphotographed at 1500× magnification in order to analyze their fine structural organization and the mitochondria number and location. Between 15 and 25 micrographs of each muscle were randomly taken at 12,000× magnification (which comprised 14,014,982 nm^2 of cell surface) to analyze the morphology of the sarcomere and sarcoplasmic reticulum (SR). Finally, at 30,000× magnification, between 10 and 20 fields were randomly microphotographed in transversal sections to evaluate actin–myosin disposition.

Morphometric measurements were performed with iTEM 5.2 (Olympus, Tokyo, Japan) for the TEM microphotographs, and analyzed using the ImageJ 1.52a program.

Micro CT scanning of one specimen was completed using an RX EasyTom (RX Solutions, Chavanod, France; http://www.rxsolutions.fr), with an aluminium filter. Images were generated at a voltage of 90 kV and a current of 333 μA, with a set frame rate of 12.5 and 5 average frames per image. This generated 5670 images and a voxel size of 20.02 μm. Reconstruction was performed using X-Act software from RX Solutions. Segmentation, visualization, and analysis were performed using Dragonfly software (Object Research Systems (ORS) Inc, Montreal, Canada, 2019; software available at http://www.theobjects.com/dragonfly). Three-dimensional (3D) images were produced in 16-bit and subsequently converted into 8-bit voxels using ImageJ (Abramoff et al., 2014). Three-dimensional processing and rendering according to the protocols reported by Zanette et al. (2014) were obtained after the semi-automatic segmentation of the body, brain, and inner ear using "generated surface." Direct volume renderings (iso-surface reconstruction) were used to visualize the subset of selected voxels of body, brain, and inner ear in AMIRA 2019.2.

2.4 | Hearing

Auditory sensitivity was determined on eleven specimens using the non-invasive auditory evoked potential (AEP) recording technique, originally reported by Kenyon et al. (Kenyon et al., 1998) and modified by Kéver et al. and Mélotte et al. (Kéver, Colleye, Herrel, et al., 2014; Mélotte et al., 2018). A Tucker-Davies Technologies (TDT, Alachua, USA) AEP workstation was used to generate sound stimuli and record AEP waveforms. TDT SigGen software was used to create sound stimuli with an RP2.1 enhanced real-time processor, a PA5 programmable attenuator to control the sound level, and a power amplifier before being sent to and emitted by the underwater speaker. Sound stimuli were tone bursts of 50 ms in duration gated with a Hanning window. The phase of the tone alternated between presentations to minimize electrical artifacts from the recordings. Thirteen frequencies were presented to each specimen: 100, 150, 300, 600, 900, 1200, 1500, 1800, 2100, 2400, 2700, 3000, and 3300 Hz. At each frequency, sound levels were presented up to 174 dB re 1 μPa and were attenuated in 6 dB steps until a threshold level was determined. At each frequency and for each sound level, the signal was presented 500 times. Evoked potentials recorded by the electrode were amplified (TDT HS4-DB4

amplifier, TDT, Alachua, USA; 10,000 gain), connected to an RP2.1 enhanced real-time processor, routed into a computer, and averaged by the BioSig software. Sound levels of the acoustic stimuli were calibrated with an HTI-96 hydrophone (Long Beach, USA; sensitivity: −163.7 dB re. 1 V μPa^{-1}; flat frequency response range between 2 Hz and 30 kHz) placed in the steel tube at the previous position of the fish's head. The hydrophone was connected to a calibrated Brüel and Kjær 2610 amplifier that gave the absolute pressure level of the sound stimuli. Evoked responses were averaged and power spectra were calculated using a 4096-point Fast Fourier Transform (FFT). The spectra were analyzed for the presence of peaks at twice the stimulus frequency with an amplitude superior to at least 3 dB above the background level. For each frequency, the lowest sound level at which such peaks were present was estimated as the auditory threshold for that frequency. A dead specimen was also tested to confirm that recorded AEP traces were not artifacts. No responses were recorded with the dead specimen.

2.5 | Statistical analysis

2.5.1 | Sounds

Descriptive statistics were realized for each variable of both kinds of sounds. For each type of sound, the mean and the standard deviation were calculated for all the acoustic variables (sound duration, period, dominant frequency, dominant amplitude, and number of peaks in the sound). The acoustic variables were first tested for the assumption of normality (Shapiro–Wilk test) and homoscedasticity of variances (*F*-test of equality of variances). Wilcoxon–Mann–Whitney tests were used to compare different acoustic variables between the two sound types. Outliers were detected thanks to Grubbs test (R package "outliers").

The link between acoustic features was examined with Spearman correlation matrices. P-values were adjusted with the Holm–Bonferroni method. To avoid pseudoreplication, the effect of the fish size on each acoustic feature was estimated with a linear mixed model (R package "nlme"; fixed effects = acoustic feature and fish size, random effect = specimen). All the statistics were carried out using R 3.3.0. (GNU General Public License) and the significance level was $\alpha = 0.05$.

2.5.2 | Histology

The measured variables were first tested for normality (Shapiro–Wilk test) and homoscedasticity of variances (*F*-test of equality of variances). According to the results, the different muscles were compared using a Kruskal–Wallis test followed by subsequent Dunn's multiple comparison test or were compared using one-way ANOVA followed by subsequent Holm–Sidak's multiple comparisons test. Ordinal variables were evaluated using the Chi-Squared test. Statistical analyses and figures were performed using R 3.3.0. (GNU General Public License) or GraphPad Prism version 7.00 for Windows. The significance level was $\alpha = 0.05$.

2.6 | Ethics

The experiments were approved by the ethical commission of the University of Liège (case 1759).

3 | RESULTS

3.1 | Acoustic signals

Two major types of sounds were recorded (Figure 1): hums and clicks. Clicks ($n_{fishes} = 6$, $n_{sounds} = 241$) lasted between 24 and 73 ms (52 ± 8 ms; mean ± SD), were made of 4–12 peaks (9 ± 1) and had a period extending from 2 to 20 ms (6 ± 2 ms). The dominant frequency ranged between 78 and 350 Hz (188 ± 34 Hz) and the sound pressure level ranged between 126 and 147 dB re 1 µPa @ 3 ± 1 cm (136 ± 4 dB re 1 µPa @ 3 ± 1 cm).

Hums ($n_{fishes} = 10$, $n_{sounds} = 75$) had a low signal to noise ratio meaning it was not easy to run the analysis. This sound type lasted between 1 and 149 s (24 ± 30 s) and was made of 55 to 7591 units (1821 ± 2672) produced at a period extending from 8 to 19 ms (14 ± 3 ms). The dominant frequency ranged between 28 and 103 Hz (75 ± 27 Hz) and the sound pressure level ranged between 62 and 131 dB re 1 µPa @ 3 ± 1 cm (89 ± 16 dB re 1 µPa @ 3 ± 1 cm).

The duration, dominant frequency, sound pressure level, and pulse period were significantly different between hums and clicks (Wilcoxon: W = 0, $p < 0.001$; W = 18,076, $p < 0.001$; W = 18,186, $p < 0.001$; W = 18,076, $p < 0.001$, respectively).

In clicks, significant positive correlations were found between the sound duration and the number of peaks ($r = 0.87$, $p < 0.001$) and between the sound pressure level and the fish total length ($r = 0.67$, $p < 0.001$). In hums, a significant positive correlation ($r = 0.66$, $p < 0.001$) was also found between the sound pressure level and the fish size (Figure 2). The linear mixed effect model showed that the sound pressure level can increase from 72 dB in small fish (45 mm TL) to 98 dB in bigger specimens (100 mm TL) for hums, and from 131 dB (60 mm TL) to 142 dB (120 mm TL) for clicks. For the two kinds of sounds, longer specimens tend to produce louder sounds.

3.2 | Hearing

Evoked potentials were obtained from all specimens tested. Representative AEP traces were similar in shape within a given test frequency across all individuals (Figure 3). Waveforms produced in response to stimulus presentation decreased in magnitude as the sound pressure level (SPL) decreased, and were thus used to determine AEP thresholds (Figure 3). AEP measurements

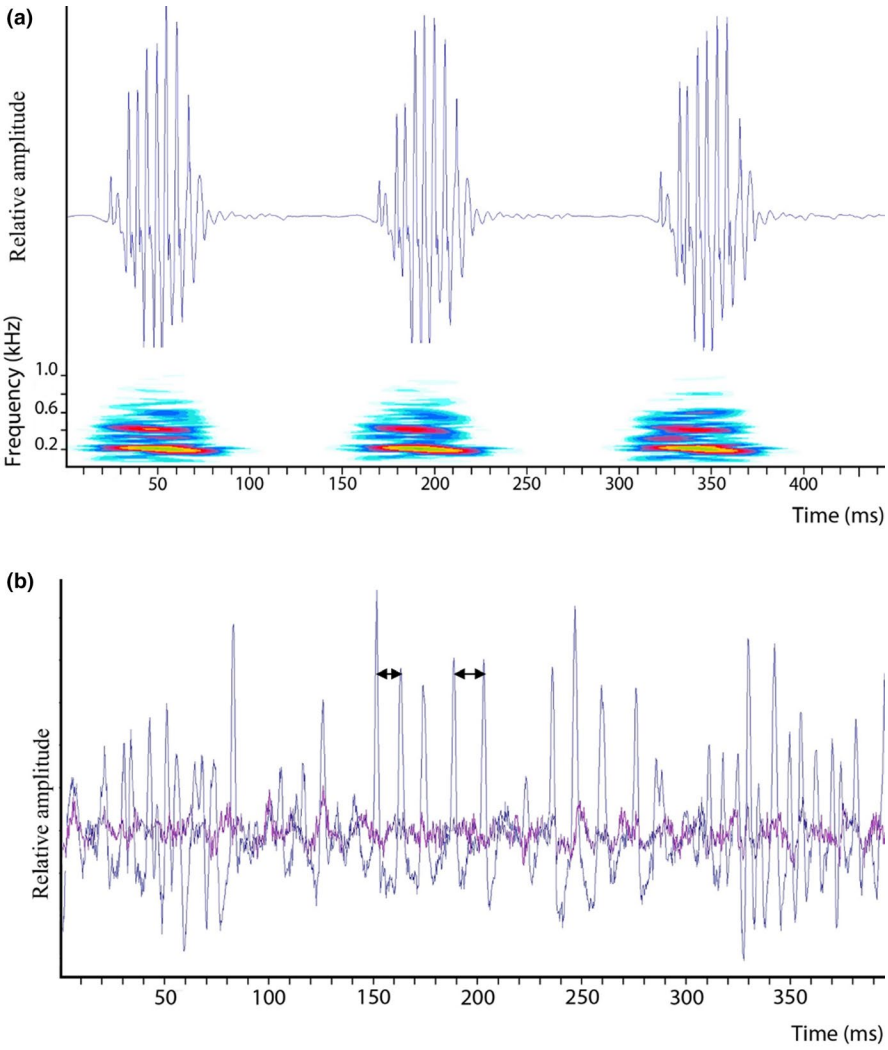

FIGURE 1 Oscillograms showing the clicks (a) and the hums (b) at different time scales in *Lactoria cornuta*. Double arrows correspond to the cycle period duration. Each pulse is made of different cycles that should correspond to a muscle contraction cycle. The purple line in B corresponds to the background noise

suggest a low sensitivity to acoustic pressure. Mean thresholds for all specimens show that they were most sensitive between 150 and 300 Hz. The sensitivity decreased regularly beyond 300 Hz, and fish cannot detect sounds higher than 2100 Hz (Figure 4). No artifacts were detected at the high sound levels when a dead fish control was run.

3.3 | Morphology

Under the rod-like vertebral column, the voluminous swim bladder extends along the entire body cavity and has two lateral rounded bumps at the anterior end (Figure 5). As was the case in *O. melea-gris* and *O. cubicus* (Parmentier et al., 2019), two elongated pterygiophores originate from the anal fin and form a vice on each side of the posterior portion of the swim bladder (Figure 5). The swim bladder wall is usually formed of two layers: the tunica interna and tunica externa. In *L. cornuta*, there is an area that is deprived of the tunica externa (Figure 5) meaning that this part of the swim bladder comprises only the tunica interna. It is called the swim bladder fenestra (SWF). In *L. cornuta*, the SWF is dorsal between the two lateral bumps and behind the vertebral column (Figure 5). In the anterodorsal part of the swim bladder, *L. cornuta* possesses two pairs of sound-producing muscles. The superficial pair is extrinsic, originating on a medial tendon that attaches to the dorsal side of the vertebral column. It covers the deep sound-producing muscle and inserts on the swim bladder wall, its fibers being perpendicular to the vertebral column. The deep pair is intrinsic to the swim bladder with muscle fibers being parallel to the vertebral column and covering the SWF. Both insertions are at the anterior and posterior ends of the SWF. In dissection, this intrinsic muscle is paler than the extrinsic one, suggesting that it is less irrigated.

3.4 | Histology

For histological analysis, both muscles attached to the swim bladder were compared to two typical skeletal muscles: an epaxial muscle (EM) and the adductor mandibulae muscle (AM). Morphological and ultrastructural characteristics of both muscles attached to the swim bladder strongly resembled features of well-characterized sonic muscles from other species. Therefore, they are referred to as

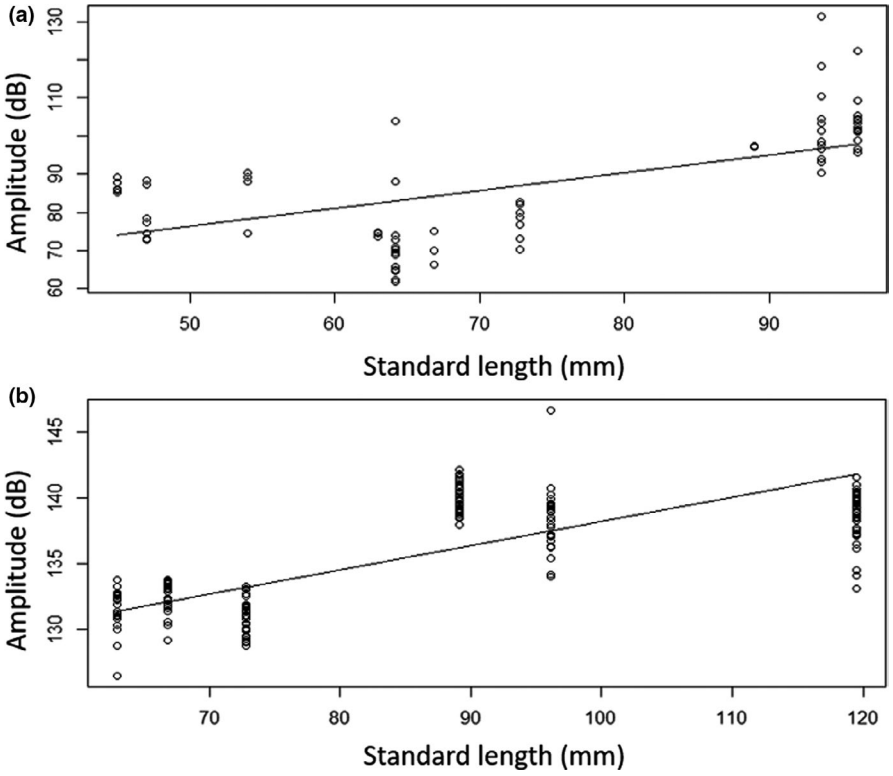

FIGURE 2 Relationship between the amplitude and the standard length for (a) hums (y = 0.46x + 53, $p = 0.031$) and (b) clicks (y = 0.18x + 120, $p = 0.034$) in *Lactoria cornuta* recorded in tank by being held in hand

extrinsic sonic muscle (ESM) and intrinsic sonic muscle (ISM) in the text below.

3.4.1 | General anatomy

In light microscopy, the fiber diameter (Figure 6), was 74 ± 17 μm for ISM, 340 ± 103 μm for ESM, 376 ± 79 μm for EM, and 349 ± 53 μm for AM (Figure 6). The diameter of ISM was statistically smaller than those of the three other muscles which were approximately equivalent (Kruskal–Wallis: $\chi^2 = 46.33$, df = 3, $p < 0.001$; Dunn: all $Z > 4.8$ and all $p < 0.001$ between ISM and the other three muscles).

Under the TEM, sound-producing muscles showed a radial morphology with alternating ribbons of sarcoplasmic reticulum (SR) and myofibrils that surrounded a central core of sarcoplasm; a subsarcolemmal ring (SSR) was also found in the periphery of the cells. Mitochondria were found in both the central core and SSR (Figure 7a). Conversely, both control muscles showed the classical anatomy of muscles with random distributions of packs of myofibrils that occupy almost all the surface, and mitochondria that are randomly dispersed all over the cell (Figure 7b). Cores and SSRs were not found in EM and AM muscles (Figure 7b) but some sarcoplasm surfaces can be found within EM. In the framework of this study, we have decided to call them core to allow comparisons between muscles. At 1200× magnification, extensive proliferation of SR was seen between myofibrils of sonic muscles, bordering sarcomeres with extremely well-developed two layered longitudinal cisternae. Triads (transversal tubes with two terminal cisternae) were found at the level of the Z-line. Between triads, the longitudinal net cisternae were less developed in EM and AM muscles than in sound-producing muscles (Figure 8).

In the transversal section, at 30,000× magnification, all four muscles showed the same arrangement of the myofilaments. Each myosin filament was surrounded by six myosin filaments in the H-zone and by six actin filaments in the A-band (Figure 8).

TEM photographs were also used for quantitative analysis to better compare the different muscles. For each muscle, 21 micrographs were taken at 1500× magnification. On each slide, extracellular space and other biological tissues (nerves, Schwann cells, capillaries, and satellite cells) were removed to work on muscle cells only. Once done, all the data were measured on similar cellular areas; that is, $6.9 \times 108\ nm^2 \pm 1.6 \times 108\ nm^2$ for ESM, $7.5 \times 108\ nm^2 \pm 2.0 \times 108\ nm^2$ for ISM, $7.6 \times 108\ nm^2 \pm 2.0 \times 108\ nm^2$ for EM, and $7.7 \times 108\ nm^2 \pm 1.4 \times 108\ nm^2$ for AM. Mathematical comparisons supported that these areas were not significantly different (one-way ANOVA: $F_{3,80} = 0.74$, $p = 0.53$), allowing comparisons.

Sonic muscles exhibited much greater sarcoplasmic spaces without myofibrils (Figure 7). In ESM and ISM, about 12.6 ± 9% and 14.5 ± 9% of the cell surface was deprived of myofibrils (myofibril-free sarcoplasm). This is rather larger than in EM (2.6 ± 1%) and AM (6 ± 4%), which means that there is more space devoted to myofibrils in both control muscles (Kruskal–Wallis: $\chi^2 = 16.68$, df = 3, $p < 0.001$) (Figure 9). Post hoc tests do not however support statistical differences between both sonic muscles and AM (ESM vs. AM, $p = 0.73$; ISM vs. AM, $p = 0.32$).

Within the cell, central cores were statistically larger (Kruskal–Wallis: $\chi^2 = 14.05$, df = 3, $p < 0.001$) in both sonic muscles

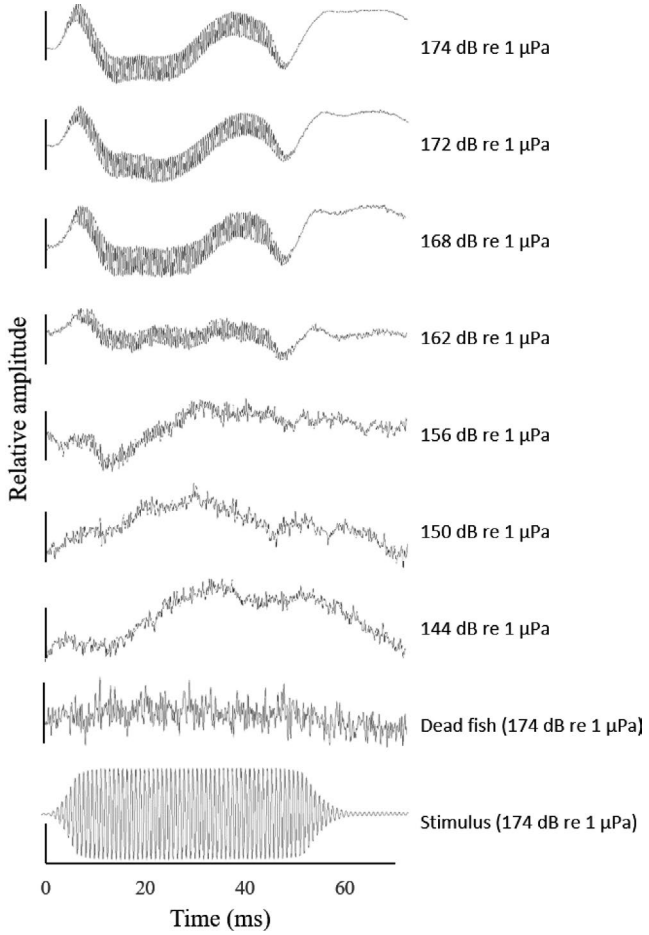

FIGURE 3 Relationship between the amplitude and the standard length for (a) hums (y = 0.46x + 53, $p = 0.031$) and (b) clicks (y = 0.18x + 120, $p = 0.034$) in *Lactoria cornuta* recorded in tank by being held in hand

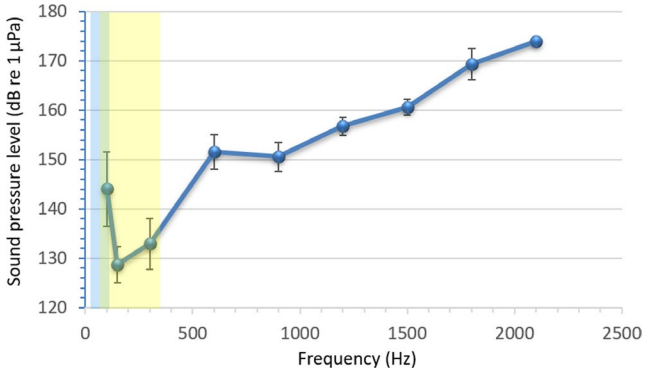

FIGURE 4 Audiogram (mean ± SD) in *Lactoria cornuta*. Yellow and blue rectangles correspond to the frequency range of clicks and hums respectively. n = 10 for all frequencies except 100 Hz (n = 7) and 2100 Hz (n = 6)

(ESM = 6.5 ± 5.6%, ISM = 11 ± 6.7%) than core in EM (1.4 ± 1%), whereas no central core was found in the adductor mandibulae (AM).

The comparison of SSR required the use of a common reference. For each kind of muscle, similar lengths of sarcolemma were measured (nm) and sarcoplasmic areas (nm^2) underlying the sarcolemma, from the sarcolemma to the packs of myofibrils, were then quantified (Figure 7). The data provide the ratio area sarcolemma^{-1} length. Higher values correspond to higher SSR space. The significant largest "ring" area of SSR was found in ISM with a ratio corresponding to 851 ± 469 (Kruskal–Wallis: $\chi^2 = 105$, df = 3, $p < 0.001$). This ratio was equivalent between other kinds of muscles (Dunn: all $Z < -0.3$ and all $p < 0.001$). It corresponded to 374 ± 239 in ESM, 268 ± 171 in EM, and 245 ± 126 in AM.

3.4.2 | Sarcomeres

Quantitative data were also collected from longitudinal sections to better study the myofibrils. These sections were extracted from micrographs at 12,000× magnification (n between 15 and 25 for each kind of muscle) for analysis of the sarcomere structures. In these longitudinal sections, the number of contractile units measured was 96 for ESM, 104 for ISM, 103 for EM, and 98 for AM. Both the H-zone and I-band were present in each sarcomere meaning muscles were all relaxed. Different measurements were taken on these longitudinal sections to characterize the sarcomeres (Table 1). ESM had the longest sarcomeres with the longest A-bands and I-bands whereas its H-bands and the myosin–actin intersection zone width were the shortest (Table 1) meaning that they were the thinnest. Sarcomere length was not statistically different between ISM and EM. The A-band length was significantly the shortest in ISM, and no statistical differences were found between other muscles (Table 1). All the I-band lengths, myosin–actin intersection zone width, and H-zone width were significantly different (Table 1).

In transversal sections, counts were made on pictures (n between 10 and 20 for each kind of muscle) at 30,000× magnification and normalized to a surface of 104 nm^2. At the level of the H-band, the lowest amount of myosin filaments was found in sonic muscles, reinforcing the fact these myofibrils were the thinnest (Table 1).

3.4.3 | Sarcoplasmic reticulum

Between 15 and 25 micrographs of each muscle at 12,000× magnification were used to analyze the sarcoplasmic reticulum. The total surface of SR was measured and expressed as the ratio of standardized cell surfaces. Both sonic muscles (ESM: 12.4 ± 5 nm^2, ISM: 12.3 ± 3.8 nm^2) presented a significantly higher area of SR (Figure 9) than both EM (6.6 ± 2.7 nm^2) and AM (4.6 ± 1.4 nm^2) (Kruskal–Wallis: $\chi^2 = 41.66$, df = 3, $p < 0.001$). SR can be divided between terminal cisternae and longitudinal sarcoplasmic cisternae. Longitudinal sarcoplasmic cisternae were statistically bigger in sonic muscles (ESM 6.2 ± 2.3 nm^2, ISM 7.1 ± 1.4 nm^2) than in EM muscle (1.6 ± 0.5 nm^2) and AM muscle (1 ± 0.4 nm^2) (one way ANOVA: $F_{3,70} = 110.3$, $p < 0.001$). There were no statistical differences between both sonic muscles. Again, surface areas were larger at the level of the surfaces of terminal cisternae in sound-producing muscles (6.1 ± 3.4 nm^2

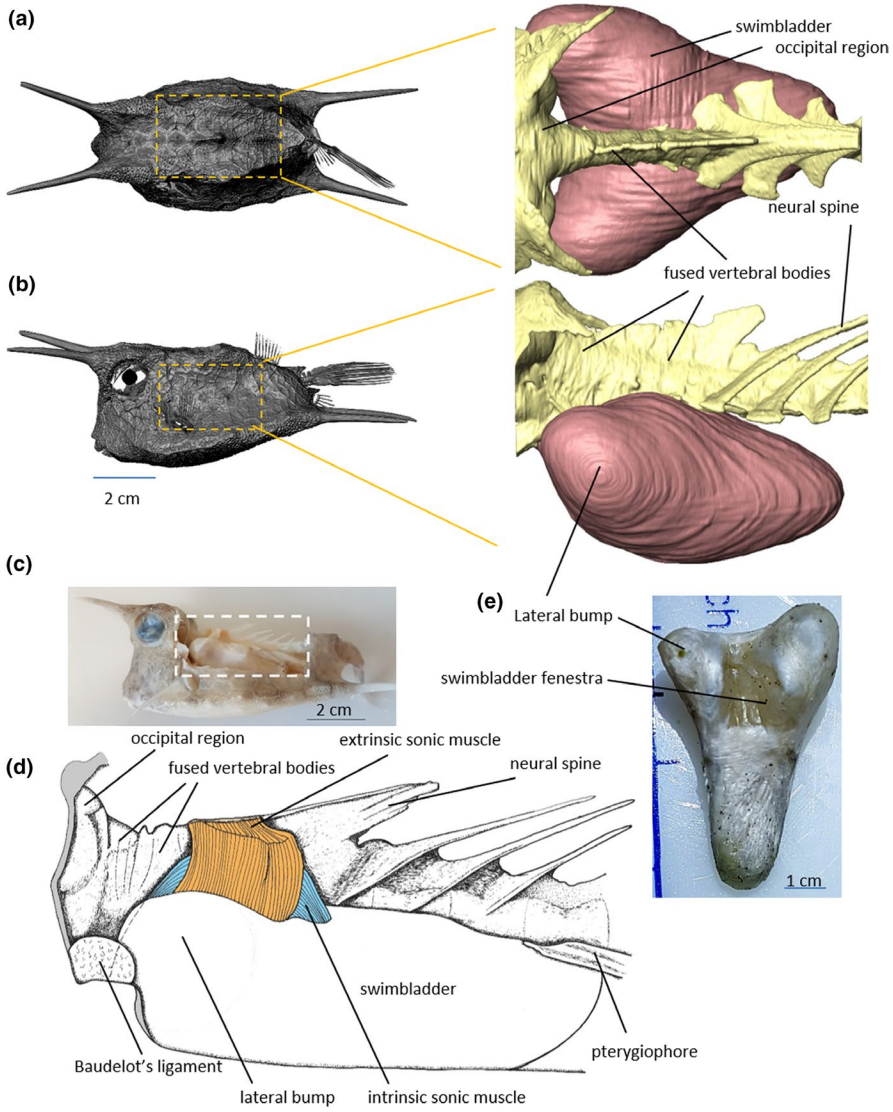

FIGURE 5 Dorsal (a) and Lateral (b) view of *Lactoria cornuta* showing the swimbladder and fused vertebrae of the vertebral column. Lateral (c, d) view of *Lactoria cornuta* showing the swimbladder and associated sound producing muscles. The drawing corresponds to the rectangle dotted line. Dorsal view of the swimbladder (e) showing the swimbladder fenestra usually hidden by vertebra and sound producing muscles. Extrinsic and Intrinsic sonic muscles are easily recognized. See the myofiber disposition is horizontal in ISM and vertical in ESM

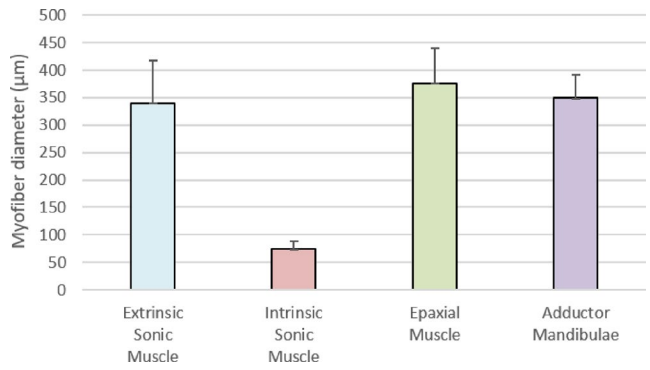

FIGURE 6 Myofiber diameters (mean ± SD) measured in different muscles in *Lactoria cornuta*. Intrinsic sonic muscle has significantly (Kruskal–Wallis = 46.33, $p < 0.001$) the thinnest cells

in ESM and 5.6 ± 1.9 nm^2 in ISM) but this difference was only significantly different from AM muscles (3.6 ± 1.2 nm^2) and not from EM muscles (4.6 ± 1.9 nm^2) (Kruskal–Wallis: $\chi^2 = 15.24$, df = 3, $p = 0.0016$).

3.4.4 | Mitochondria

The number of mitochondria was analyzed in microphotographs (n = 21 for each muscle) at 1500× magnification. Sonic muscles presented a significantly higher number of mitochondria compared to controls; 502 mitochondria in ESM, 553 in ISM, 215 in EM, and 321 in AM (Kruskal–Wallis: $\chi^2 = 186.7$, df = 3, $p < 0.0001$).

4 | DISCUSSION

As was previously described in the boxfishes *Ostracion meleagris* and *O. cubicus* (Parmentier et al., 2019), *Lactoria cornuta* can produce (at least) two different kinds of sounds: hums and clicks that have an average dominant frequency of 75 and 188 Hz, respectively. They also possess two pairs of sound-producing muscles (ESM and ISM) attached to the swim bladder. Fish that have muscles inserting on the swim bladder can be roughly separated into two groups. The first group corresponds to the *rebound model*: these fish possess slow muscles that stretch the swim bladder and

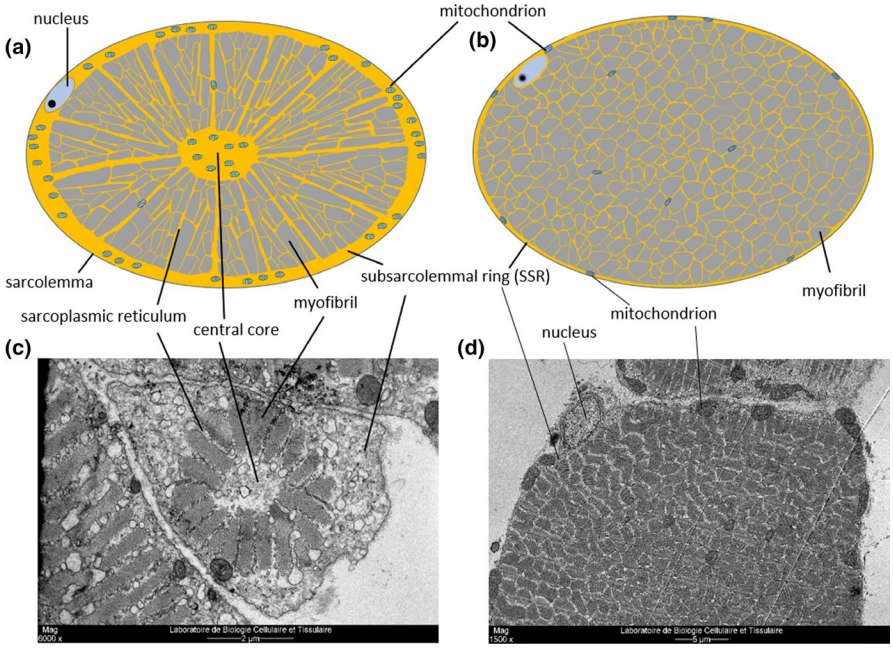

FIGURE 7 Schematic drawings of the intrinsic sound producing muscle (a) and control skeletal muscle (b) in *Lactoria cornuta*, TEM microphotographs of a transversal section of intrinsic sonic muscle (c) and adductor muscle (d). In a and b, ratio correspond at best to quantitative data

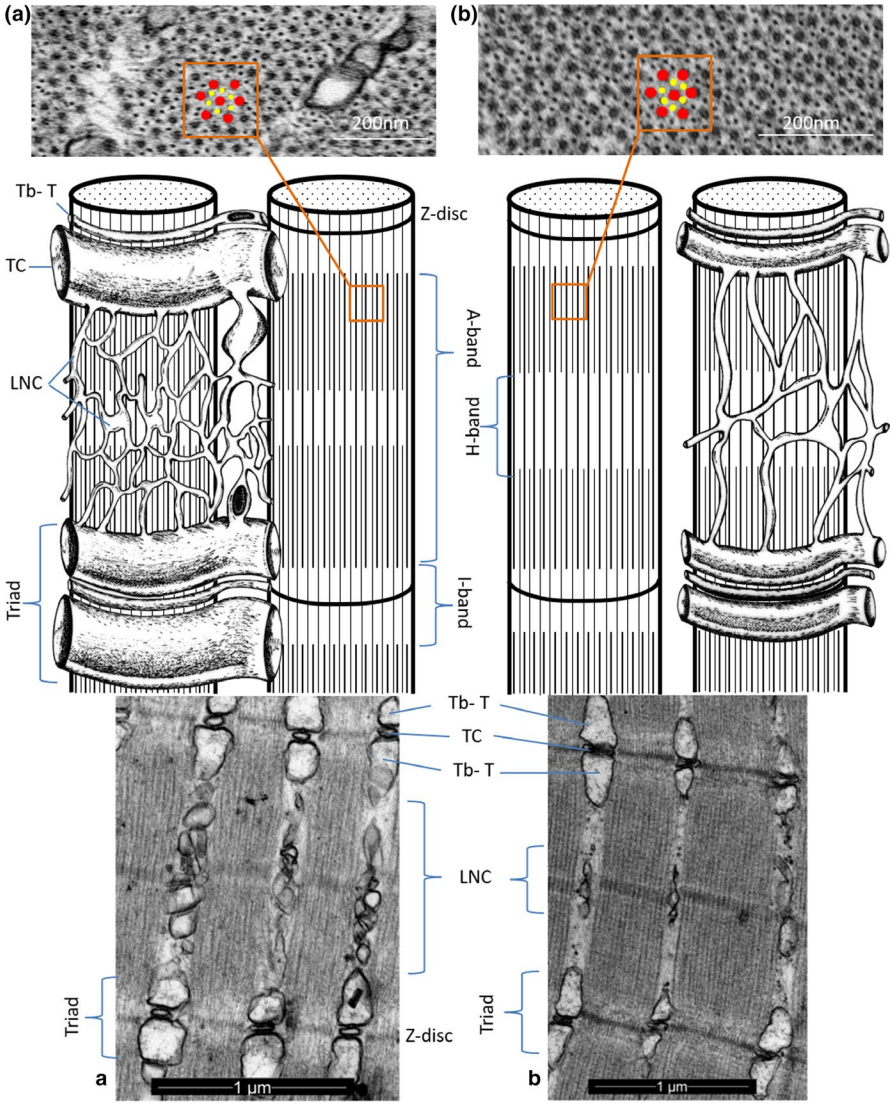

FIGURE 8 Reconstruction of the intrinsic sound producing muscle (a) and epaxial (b) with TEM microphotographs of myofibrils showing myosin (red) and actin (yellow) filaments, and longitudinal sections showing sarcomeres and cisternae in corresponding muscles. Please note band lengths are proportional. Tb-T: tubule T; TC: terminal cisternae; LNC: longitudinal net cisternae

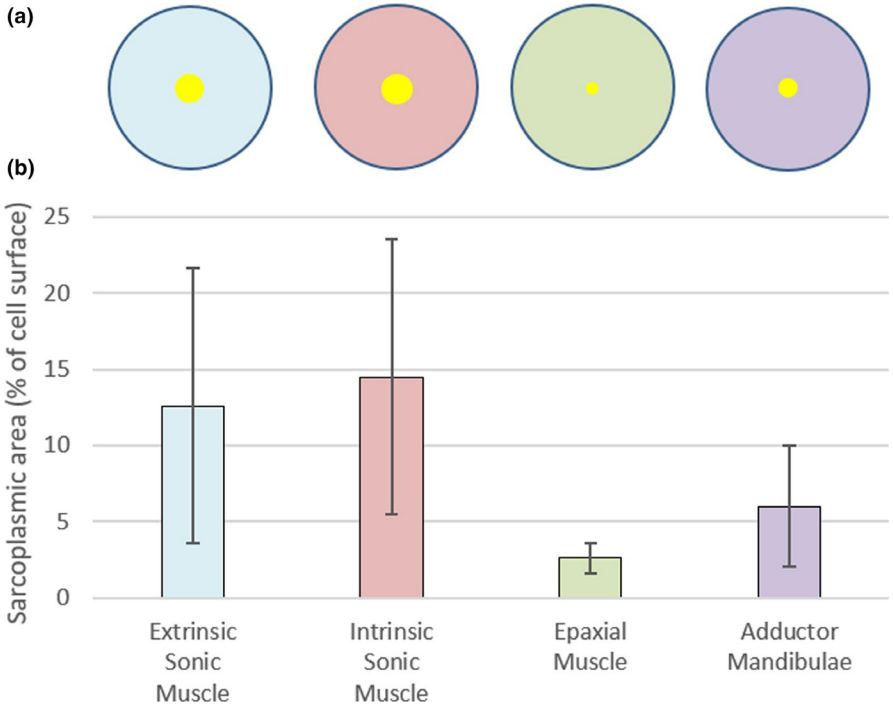

FIGURE 9 Total sarcoplasmic spaces without myofibrils in four muscles of *Lactoria cornuta*. (a) All the muscle sections are placed at the same scale and the yellow circle corresponds to the space part without myofibrils. (b) Histogram (mean ± SD) showing the total sarcoplasmic space. Both sonic muscles presented a significantly higher area of than both control muscles (Kruskal–Wallis: $\chi^2 = 41.66$; $p < 0.001$)

	ESM	ISM	EM	AM
Sarcomere length (nm)	1829 ± 150†‡§	1712 ± 126*§	1708 ± 78*§	1750 ± 99*†‡
A-band length (nm)	1453 ± 130†	1344 ± 91*‡§	1431 ± 67†	1430 ± 101†‡
I-band length (nm)	418 ± 102†‡§	368 ± 78*‡§	275 ± 30*†§	328 ± 52*†‡
H-band width (nm)	277 ± 77†‡§	353 ± 78*‡§	462 ± 173*†§	665 ± 244*†‡
myosin–actin intersection zone width (nm)	321 ± 73†‡§	401 ± 87*‡§	499 ± 166*†§	728 ± 251*†‡
Ratio I-band/A-band	0.27 ± 0.06‡§	0.27 ± 0.06‡§	0.19 ± 0.02*†§	0.23 ± 0.04*†‡
H zone myosin filaments	6.9 ± 1†§	6 ± 0.4*‡§	7.1 ± 0.7†§	8.2 ± 1*†‡

TABLE 1 Morphometric data from different muscles in the longitudinal section in *Lactoria cornuta*. These data were used to build Figure 8. Mean ± SD. Signs denote significant differences ($p < 0.05$) from ESM (*), ISM (†), EM (‡), and AM (§).

79.4 78.5 83 81.
15 20.6 27 38.

associated tendons, allowing sound production by the rebound of the swim bladder wall and associated bones (Kéver, Colleye, Lugli, et al., 2014; Mok et al., 2011; Parmentier, Bouillac, et al., 2010; Parmentier, Fabri, et al., 2010; Parmentier et al., 2006). In this first group, the muscle contraction rate corresponds to the pulse period but not to the fundamental frequency (Parmentier et al., 2019). In the second group, the dominant frequency corresponds to the muscle contraction rate and to the peak period within each pulse. Therefore, each pulse within each sound could result from regular groups of one to five muscle contractions (Figure 1). This is the case in *L. cornuta*.

This kind of sound-producing mechanism corresponds to the *forced-response model* where the frequency usually reflects the muscle contraction rate (Fine et al., 2001; Millot et al., 2011), suggesting *de facto* that both muscles are fast-contracting muscles. These fast sonic muscles are known to produce a steady and constant displacement of the swim bladder that allows sound generation (Millot et al., 2011; Parmentier et al., 2014). Because species that possess this kind of mechanism are not phylogenetically related, sound production with fast muscles appears to be a nice case of evolutionary convergence where constraints, for example highly damped swim bladder wall (Fine et al., 2016), are solved in the same way.

The results of this study on the longhorn cowfish are important because they highlight the fact that, having two muscles with different orientations and insertions on the swim bladder, the whole system can be subject to plasticity. Although solutions all require rapid bladder movement the required conditions to make sounds are not strict and are not related to the swim bladder shape or to the muscle

orientation. These few required conditions nicely illustrate that the system has evolved many times in distant taxa.

The hypothesis dealing with fast contractions is well supported by a set of morphological features which are usually found in fast contracting sonic muscles (Appelt et al., 1991; Boyle et al., 2015; Eichelberg, 1976, 1977; Kéver, Boyle, et al., 2014) that can operate at high rates, between 80 and 300 Hz (Boyle et al., 2015; Eichelberg, 1976, 1977; Fine et al., 1990; Millot & Parmentier, 2014; Parmentier & Diogo, 2006): small cell diameter, peculiar myofibrillar organization with alternating ribbons of sarcoplasmic reticulum and myofibrils radiating out from a core of sarcoplasm, vast sarcoplasmic surfaces without myofibrils (including the peripheral ring) and numerous mitochondria. This organization is thought to guarantee easy dissemination of ATP, calcium ions and other substrates (Eichelberg, 1976; Fine et al., 1990; Ono & Poss, 1982). Conversely, epaxial and adductor mandibulae are morphologically typical of slow-twitch muscles: cytoplasm is almost completely dedicated to myofibrils with few mitochondria placed between them (Schiaffino & Reggiani, 2011).

The ratio I-band length/A-band length is higher in sonic muscles, showing that the I-band component is highly responsible for the total sarcomere length. It also means there is more overlap surface between actin and myosin filaments. As the force generated by a muscle depends on the number of actin and myosin cross-bridges formed, a larger number of cross-bridges should provide more force/sarcomere in these muscles. Consequently, fast sonic muscle sarcomere architecture in *L. cornuta* could be designed to produce stronger contractions that counterbalance or attenuate the smaller number of myofibrils. In the comparison between muscles, ESM should provide more force than ISM because its sarcomeres are longer (1.83 μm vs. 1.71 μm, Table 1). Because the I-band length is close to the sarcomere length in sound-producing muscles, myofilaments remain almost constant during contraction, suggesting that they are both qualified to generate short contractions.

However, there are differences between sound types. Hums are long sounds made of trains of low amplitude pulses and results from multiple contractions, suggesting that they are produced by fatigue-resistant muscles. Clicks correspond to shorter sounds with greater amplitude than in the hums, suggesting that they result from more powerful contractions.

The main components of muscle fibers are myofibrils, SR, and mitochondria in varying proportions (Figure 10). The volume occupied by myofibrils determines the force of contraction, the volume of sarcoplasmic reticulum can reflect the contraction frequency, whereas the volume of mitochondria sets the level of sustained performance (Lindstedt et al., 1998). Variations in these components' proportions can provide the muscle with different kinds of performance that are mutually exclusive (Rome et al., 1999). In a given space, any increase in one structure (and its concomitant function), must be to some extent at the expense of another (Lindstedt et al., 1998). An investment in force (corresponding to many myofibrils) cannot take place simultaneously with an investment in speed (corresponding to high volume devoted to SR). This is precisely the situation with fast sound-producing muscle that can contract at high rates but in this case develops low force

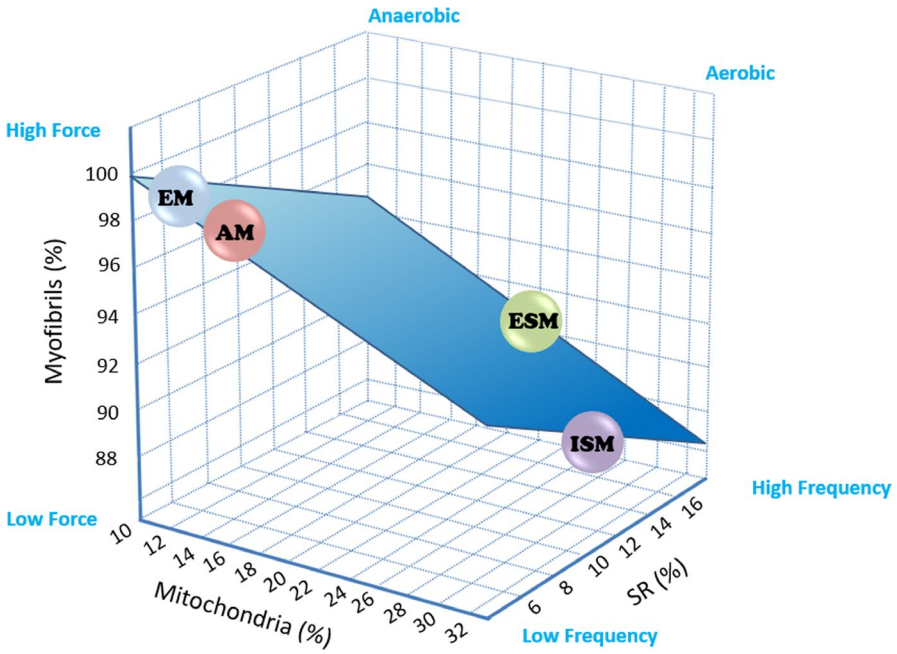

FIGURE 10 Three-dimensional plot of *Lactoria cornuta* muscle profiles according to the relationship between the principal constituents that determine the properties of muscular fibers: myofibril volume (contraction force), amount of mitochondria (cellular metabolism), and SR volume (contraction/relaxation frequency). Bubbles represent group mean values of each of the muscles analysed. This figure shows how both sonic muscles are located at the edge of the graphic in which the force is weak, the frequency is elevated and aerobic metabolisms takes part. On the opposite extreme of the plane, skeletal control muscles exhibited high force, an anaerobic metabolism and low frequency. For details see text. This graphic was adapted from Rome et al. (1999)

(Lindstedt et al., 1998; Rome et al., 1996, 1999). Moreover, mitochondria are known to provide ATP which is used for cross-bridge activation and for Ca^{2+} pumping at the level of the sarcoplasmic reticulum. Consequently, the amount of mitochondria determines the magnitude of the sustainable performance of the muscle (Figure 10); therefore, the total volume of mitochondria is an accurate predictor of muscle aerobic capacity (Lindstedt et al., 1998; Rome & Lindstedt, 1998). It is supposed that all mitochondria from the central core and in-between myofibrils participate in muscle contraction with the actin–myosin cross-bridge and calcium cycle. All other mitochondria could be involved in other cell functions.

Although ESM and ISM cells are smaller, mitochondria were statistically more numerous in sonic muscles than in EP and AM which is usually the case in this kind of muscle (Appelt et al., 1991; Fine et al., 1993). The same pattern can be found in fast muscles of flying insects, of rattlesnake tails, and different sonic muscles in teleosts (Conley & Lindstedt, 1996; Rome & Lindstedt, 1998). It suggests that both sound-producing muscles should operate their contraction reactions using ATP produced by oxidative phosphorylation and have high muscle aerobic capacity giving better resistance to fatigue.

In addition to mitochondrial volume density being high, perhaps the most obvious structural characteristic of fast sound-producing fibers is the exceptionally high volume density of SR (Boyle et al., 2015; Fawcett & Revel, 1961; Feher et al., 1998). In *L. cornuta*, the sarcoplasmic reticulum volume is higher in sonic muscles than in control muscles (Figure 10). There are two apparent consequences of a high SR density that can explain high-speed characteristics. First, there are multiple sites for Ca^{2+} uptake, which is likely to ensure both rapid muscle contraction and relaxation. Second, the distance between the SR and the cross-bridges is minimized, ensuring simultaneous activation of the whole muscle. Thus, the combination of a very high density of SR coupled with small packs of myofibrils is ideally suited for rapid activation and relaxation. By cycling Ca^{2+} rapidly, the muscle can be activated nearly instantaneously, while the high density of SR also ensures that it relaxes rapidly to prepare for the next twitch. In other words, the SR surface determines the contraction rate that a cell is capable of achieving (Mead et al., 2017).

Finally, this study showed that *L. cornuta* was sensitive to frequencies ranging between at least 100 and 400 Hz with thresholds of 128–143 dB re 1 μPa over this range, meaning that they are more sensitive to the frequencies produced by conspecifics. More precisely, it seems that fish can easily detect the clicks but the hums are harder to detect. However, three remarks must be made. (1) Classical underwater loudspeakers do not allow testing of frequencies below 100 Hz, limiting the interpretation. (2) AEP threshold techniques may underestimate behavioral thresholds by 10–30 dB, especially at frequencies of <1 kHz (Kenyon et al., 1998; Kojima et al., 2005). (3) Sound amplitude seems to be related to fish size (Figure 2). In this species, adults can grow to 400 mm and the biggest specimens we encountered were 120 mm long. According to this relationship, it will be easier for *L. cornuta* specimens to detect hums from longer specimens. It also implies that sounds should provide information on the size of the sound producer (Parmentier & Fine, 2016).

5 | CONCLUSION

Ultra-structural differences are found between ESM and ISM. According to features such as long sarcomeres, long I-bands, high number of mitochondria, and huge amount of SR, ESM would be able to produce fast, strong, and short contractions. Accordingly, ESM should produce clicks that are the shortest sounds with greatest amplitude. ISM shows the thinnest cells, the smallest number of myofilaments that have long I-bands, the highest volume of mitochondria, and well-developed SR. All these features support that ISM should generate fast and prolonged contractions because they are fatigue resistant. ISM should produce the hums that are long sounds made of trains of low amplitude pulses over long periods of time. This study also shows that AM and EM present ultra-structural characteristics of powerful muscles. As myofibril volume, SR volume, and mitochondria volume collectively make up essentially 100% of the fiber, every muscle fiber is identifiable as a point on a single plane of a three-dimensional graph depicting these muscle components (Lindstedt et al., 1998; Rome & Lindstedt, 1998).

ACKNOWLEDGMENTS

Marie Bournonville and the team from the Museum-Aquarium (Liège, Belgium) kindly helped with fish maintenance. Dominique Mallevoy and the team of Nausicaa (Boulogne Sur Mer, France) allowed us to test their specimens. We thank Jonathan Brecko (RBINS, Bruxelles, Belgium) for CT-scanning the specimens. Michael Fine and another referee help to improve the text.

CONFLICTS OF INTEREST

The authors do not have any conflicts of interest to declare.

AUTHORS' CONTRIBUTIONS

EP and MT conceived and designed the experiments. MM and XR performed hearing experiments and sound analysis. EP performed the CT scan, 3D constructions, and the study of the anatomy. EMF and MT performed histological study. EMF, MM, and XR performed statistical analysis. EP wrote the manuscript; other authors provided editorial advice.

DATA AVAILABILITY STATEMENT

The data that support the findings of this study are available from the corresponding author upon reasonable request.

ORCID

Eric Parmentier https://orcid.org/0000-0002-0391-7530
Xavier Raick https://orcid.org/0000-0002-1977-0289

REFERENCES

Abramoff, M.D., Magalhaes, P.J. & Ram, S.J. (2014) Image processing with ImageJ. *Biophotonics International*, 11, 36–42.

Akamatsu, T., Okumura, T., Novarini, N. & Yan, H.Y. (2002) Empirical refinements applicable to the recording of fish sounds in small tanks. *Journal of the Acoustical Society of America*, 112, 3073–3082.

Appelt, D., Shen, V. & Franzini-Armstrong, C. (1991) Quantitation of Ca ATPase, feet and mitochondria in superfast muscle fibres from the toadfish, *Opsanus tau*. *Journal of Muscle Research and Cell Motility*, 12, 543–552.

Boyle, K.S., Colleye, O. & Parmentier, E. (2014) Sound production to electric discharge: Sonic muscle evolution in progress in *Synodontis* spp. catfishes (Mochokidae). *Proceedings of the Royal Society B-Biological Sciences*, 281, 1197.

Boyle, K.S., Riepe, S., Bolen, G. & Parmentier, E. (2015) Variation in swim bladder drumming sounds from three doradid catfish species with similar sonic morphologies. *Journal of Experimental Biology*, 218, 2881–2891.

Bridge, T.W. (1904) Fishes. In: Harmer, S.F. and Shipley, A.E. (Eds.) *The Cambridge natural history*. London: Macmillan and Co, pp. 139–727.

Conley, K.E. & Lindstedt, S.L. (1996) Minimal cost per twitch in rattlesnake tail muscle. *Nature*, 383, 71–72.

Eichelberg, H. (1976) The fine structure of the drum muscles of the tigerfish, *Therapon jarbua*, as compared with the trunk musculature. *Cell and Tissue Research*, 174, 453–463.

Eichelberg, H. (1977) Fine structure of the drum muscles of the piranha (Serrasalminae, Characidae). *Cell and Tissue Research*, 185, 547–555.

Fawcett, D.W. & Revel, J.P. (1961) The sarcoplasmic reticulum of a fast-acting fish muscle. *The Journal of Biophysical and Biochemical Cytology*, 10, 89–109.

Feher, J., Waybright, T. & Fine, M. (1998) Comparison of sarcoplasmic reticulum capabilities in toadfish (*Opsanus tau*) sonic muscle and rat fast twitch muscle. *Journal of Muscle Research and Cell Motility*, 19, 661–674.

Fine, M.L., Bernard, B. & Harris, T.M. (1993) Functional morphology of toadfish sonic muscle fibers: Relationship to possible fiber division. *Canadian Journal of Zoology*, 71, 2262–2274.

Fine, M.L., Burns, N.M. & Harris, T.M. (1990) Ontogeny and sexual dimorphism of sonic muscle in the oyster toadfish. *Canadian Journal of Zoology*, 68, 1374–1381.

Fine, M.L., King, T.L., Ali, H., Sidker, N. & Cameron, T.M. (2016) Wall structure and material properties cause viscous damping of swimbladder sounds in the oyster toadfish *Opsanus tau*. *Proceedings of the Royal Society B-Biological Sciences*, 283, 20161094.

Fine, M.L., Malloy, K.L., King, C., Mitchell, S.L. & Cameron, T.M. (2001) Movement and sound generation by the toadfish swimbladder. *Journal of Comparative Physiology A*, 187, 371–379.

Fine, M.L. & Parmentier, E. (2015) Mechanisms of sound production. In: Ladich, F. (Ed.) *Sound communication in fishes*. Wien: Springer, pp. 77–126.

Fish, M.P. (1948). Sonic fishes of the Pacific (technical report no. 2). Woods Hole Oceanographic Institution, Woods Hole, MA.

Fish, M.P. & Mowbray, H.M. (1970) *Sounds of western north Atlantic fishes*. Baltimore, MD: The Johns Hopkins Press.

Heyd, A. & Pfeiffer, W. (2000) Über die Lauterzeugung der Welse (Siluroidei, Ostariophysi, Teleostei) und ihren Zusammenhang mit der Phylogenese und der Schreckreaktion. *Revue Suisse de Zoologie*, 107, 165–211.

Kenyon, T.N., Ladich, F. & Yan, H.Y. (1998) A comparative study of hearing ability in fishes: The auditory brainstem response approach. *Journal of Comparative Physiology A*, 182, 307–318.

Kéver, L., Boyle, K.S., Dragičević, B., Dulčić, J. & Parmentier, E. (2014) A superfast muscle in the complex sonic apparatus of *Ophidion rochei* (Ophidiiformes): Histological and physiological approaches. *Journal of Experimental Biology*, 217, 3432–3440.

Kéver, L., Colleye, O., Herrel, A., Romans, P. & Parmentier, E. (2014) Hearing capacities and otolith size in two ophidiiform species (*Ophidion rochei* and *Carapus acus*). *Journal of Experimental Biology*, 217, 2517–2525.

Kéver, L., Colleye, O., Lugli, M., Lecchini, D., Lerouvreur, F., Herrel, A. & et al. (2014) Sound production in *Onuxodon fowleri* (Carapidae) and its amplification by the host shell. *Journal of Experimental Biology*, 217, 4283–4294.

Kojima, T., Ito, H., Komada, T., Taniuchi, T. & Akamatsu, T. (2005) Measurements of auditory sensitivity in common carp *Cyprinus carpio* by the auditory brainstem response technique and cardiac conditioning method. *Fisheries Science*, 71, 95–100.

Ladich, F. (1997) Comparative analysis of swimbladder (drumming) and pectoral (stridulation) sounds in three families of catfishes. *Bioacoustics*, 8, 185–208.

Ladich, F. & Bass, A.H. (2005) Sonic motor pathways in piranhas with a reassessment of phylogenetic patterns of sonic mechanisms among teleosts. *Brain, Behavior and Evolution*, 66, 167–176.

Ladich, F. & Fine, M.L. (2006) Sound-generating mechanisms in fishes: A unique diversity in vertebrates. In: Ladich, F., Collin, S.P., Moller, P. and Kapoor, B.G. (Eds.) *Communication in fishes*. Enfield, NH: Science Publishers, pp. 3–34.

Lindstedt, S.L., McGlothlin, T., Percy, E. & Pifer, J. (1998) Task-specific design of skeletal muscle: Balancing muscle structural composition. *Comparative Biochemistry and Physiology Part B: Biochemistry and Molecular Biology*, 120, 35–40.

Lobel, P.S. (1996) Spawning sound of the trunkfish, *Ostracion meleagris* (Ostraciidae). *Biological Bulletin*, 191, 308–309.

Loesser, K.E., Ra, J. & Fine, M.L. (1997) Embryonic, juvenile, and adult development of the toad sonic muscle. *Anatomical Record*, 249, 469–477.

Mann, D.A. & Lobel, P.S. (1995) Passive acoustic detection of sounds produced by the damselfish, *Dascyllus albisella* (Pomacentridae). *Bioacoustics*, 6, 199–213.

Markl, H. (1971) Schallerzeugung bei Piranhas (Serrasalminae, Characidae). *Zeitschrift für Vergleichende Physiologie*, 74, 39–56.

Mead, A.F., Osinalde, N., Ørtenblad, N., Nielsen, J., Brewer, J., Vellema, M. et al. (2017) Fundamental constraints in synchronous muscle limit superfast motor control in vertebrates. *Elife*, 6, e29425.

Mélotte, G., Parmentier, E., Michel, C., Herrel, A. & Boyle, K. (2018) Hearing capacities and morphology of the auditory system in Serrasalmidae (Teleostei: Otophysi). *Scientific Reports*, 8, 1281.

Mélotte, G., Raick, X., Vigouroux, R. & Parmentier, E. (2019) Origin and evolution of sound production in Serrasalmidae. *Biological Journal of the Linnean Society*, https://doi.org/10.1093/biolinnean/blz105

Mélotte, G., Vigouroux, R., Michel, C. & Parmentier, E. (2016) Interspecific variation of warning calls in piranhas: A comparative analysis. *Scientific Reports*, 6, 36127.

Millot, S. & Parmentier, E. (2014) Development of the ultrastructure of sonic muscles: A kind of neoteny? *BMC Evolutionary Biology*, 14, 1–9.

Millot, S., Vandewalle, P. & Parmentier, E. (2011) Sound production in red-bellied piranhas (*Pygocentrus nattereri*, Kner): An acoustical, behavioural and morphofunctional study. *Journal of Experimental Biology*, 214, 3613–3618.

Mok, H.-K., Parmentier, E., Chiu, K.-H., Tsai, K.-E., Chiu, P.-H. & Fine, M.L. (2011) An intermediate in the evolution of superfast sonic muscles. *Frontiers in Zoology*, 8, 31.

Moyer, J.T. (1979) Mating strategies and reproductive behavior of ostraciid fishes at Miyake-jima, Japan. *Japanese Journal of Ichthyology*, 26, 148–160.

Ono, R.D. & Poss, S.G. (1982) Structure and innervations of the swimbladder musculature in the weakfish, *Cynoscion regalis* (Teleostei: Sciaenidae). *Canadian Journal of Zoology*, 60, 1955–1967.

Onuki, A. & Somiya, H. (2004) Two types of sounds and additional spinal nerve innervation to the sonic muscle in John Dory, *Zeus faber* (Zeiformes: Teleostei). *Journal of the Marine Biological Association of the United Kingdom*, 84, 843–850.

Parmentier, E., Bahri, M.A., Plenevaux, A., Fine, M.L. & Estrada, J.M. (2018) Sound production and sonic apparatus in deep-living cusk-eels (*Genypterus chilensis* and *Genypterus maculatus*). *Deep Sea Research Part I: Oceanographic Research Papers*, 141, 83–92.

Parmentier, E., Bouillac, G., Dragicevic, B., Dulcic, J. & Fine, M. (2010) Call properties and morphology of the sound-producing organ in *Ophidion rochei* (Ophidiidae). *Journal of Experimental Biology*, 213, 3230–3236.

Parmentier, É., Colleye, O. & Lecchini, D. (2016) New insights into sound production in *Carapus mourlani* (Carapidae). *Bulletin of Marine Science*, 92.

Parmentier, E. & Diogo, R. (2006) Evolutionary trends of swimbladder sound mechanisms in some teleost fishes. In: Ladich, F., Collin, S.P., Moller, P. and Kapoor, B.G. (Eds.) *Communication in fishes*. Enfield, NH: Science Publishers, pp. 45–70.

Parmentier, E., Fabri, G., Kaatz, I., Decloux, N., Planes, S. & Vandewalle, P. (2010) Functional study of the pectoral spine stridulation mechanism in different mochokid catfishes. *Journal of Experimental Biology*, 213, 1107–1114.

Parmentier, E. & Fine, M.L. (2016) Fish sound production: Insights. In: Suthers, R., Tecumseh, F., Popper, A.N. and Fay, R.R. (Eds.) *Vertebrate sound production and acoustic communication*. Springer, pp. 19–49.

Parmentier, E., Fine, M.L., Berthe, C. & Lecchini, D. (2018) Taxonomic validation of Encheliophis chardewalli with description of calling abilities. *Journal of Morphology*, 279, 864–870.

Parmentier, E., Lagardère, J.-P., Braquegnier, J.-B., Vandewalle, P. & Fine, M.L. (2006) Sound production mechanism in carapid fish: First example with a slow sonic muscle. *Journal of Experimental Biology*, 209, 2952–2960.

Parmentier, E., Raick, X., Lecchini, D., Boyle, K., Vanwassenbergh, S., Bertucci, F. & et al. (2017) Unusual sound production mechanism in the triggerfish *Rhinecanthus aculeatus* (Balistidae). *Journal of Experimental Biology*, 220, 186–193.

Parmentier, E., Solagna, L., Bertucci, F., Fine, M.L., Nakae, M., Compère, P. et al. (2019) Simultaneous production of two kinds of sounds in relation with sonic mechanism in the boxfish *Ostracion meleagris* and *O. cubicus*. *Scientific Reports*, 9, 4962.

Parmentier, E., Tock, J., Falguière, J.-C. & Beauchaud, M. (2014) Sound production in *Sciaenops ocellatus*: Preliminary study for the development of acoustic cues in aquaculture. *Aquaculture*, 432, 204–211.

Raick, X., Lecchini, D., Kéver, L., Colleye, O., Bertucci, F. & Parmentier, É. (2018) Sound production mechanism in triggerfish (Balistidae): A synapomorphy. *The Journal of Experimental Biology*, 221(1), jeb168948.

Rome, L.C., Cook, C., Syme, D.A., Connaughton, M.A., Ashley-Ross, M., Klimov, A. et al. (1999) Trading force for speed: Why superfast crossbridge kinetics leads to superlow forces. *Proceedings of the National Academy of Sciences of the United States of America*, 96, 5826–5831.

Rome, L.C. & Lindstedt, S.L. (1998) The quest for speed: Muscles built for high-frequency contractions. *News in Physiological Sciences*, 13, 261–268.

Rome, L.C., Syme, D.A., Hollingworth, S., Lindstedt, S.L. & Baylor, S.M. (1996) The whistle and the rattle: The design of sound producing muscles. *Proceedings of the National Academy of Sciences of the United States of America*, 93, 8095–8100.

Santini, F., Sorenson, L., Marcroft, T., Dornburg, A. & Alfaro, M.E. (2013) A multilocus molecular phylogeny of boxfishes (Aracanidae, Ostraciidae; Tetraodontiformes). *Molecular Phylogenetics and Evolution*, 66, 153–160.

Schiaffino, S. & Reggiani, C. (2011) Fiber types in mammalian skeletal muscles. *Physiological Reviews*, 91, 1447–1531.

Schneider, H. (1961) Neuere Ergebnisse der Lautforschung bei Fischen. *Naturwissenschaften*, 48, 513–518.

Tellechea, J.S., Teixera-de Mollo, F., Gonzalez-Bergonzoni, I. & Vidal, N. (2011) Sound production and pectoral spine locking in a Neotropical catfish (*Iheringichthys labrosus*, Pimelodidae). *Neotropical Ichthyology*, 9, 889–894.

Uchida, K. (1934) Sound producing fish of Japan. *Rep. Japan Sci. Assoc.*, 9, 369–375.

Zanette, I., Daghfous, G., Weitkamp, T., Gillet, B. & Adriaens, D. (2014) Looking inside marine organisms with magnetic resonance and X-ray imaging. *Imaging marine life: Macrophotography and microscopy approaches for marine biology*. pp. 123–184.

How to cite this article: Parmentier E, Marucco Fuentes E, Millot M, Raick X, Thiry M. Sound production, hearing sensitivity, and in-depth study of the sound-producing muscles in the cowfish (*Lactoria cornuta*) *J. Anat*. 2020;00:1–14. https://doi.org/10.1111/joa.13353